The American Journal of Pathology, Vol. 171, No. 6, December 2007

DOI: 10.2353/ajpath.2007.070261

Epithelial and Mesenchymal Cell Biology

Loss of Partitioning-Defective-3/Isotype-Specific Interacting Protein (Par-3/ASIP) in the Elongating Spermatid of RA175 (IGSF4A/SynCAM)-Deficient Mice

Eriko Fujita,* Yuko Tanabe,*† Tomonori Hirose,‡ Michel Aurrand-Lions,§ Tadashi Kasahara,† Beat A. Imhof,§ Shigeo Ohno,‡ and Takashi Momoi*

From the Division of Differentiation and Development, Department of Inherited Metabolic Disorder, National Institute of Neuroscience, National Center of Neurology and Psychiatry, Tokyo, Japan; the Department of Biochemistry,† Kyoritsu University of Pharmacy, Tokyo, Japan; the Department of Molecular Biology,‡ Yokohama City University Graduate School of Medical Science, Yokohama City University School of Medical Science, Yokohama, Japan; and the Department of Pathology and Immunology,§ University of Geneva, Geneva, Switzerland*

IGSF4a/RA175/SynCAM (RA175) and junctional adhesion molecules (Jams) are members of the immunoglobulin superfamily with a PDZ-binding domain at their C termini. Deficiency of *Ra175* (*Ra175*$^{-/-}$) as well as *Jam-C* deficiency (*Jam-C*$^{-/-}$) causes the defect of the spermatid differentiation, oligo-astheno-teratozoospermia. *Ra175*$^{-/-}$ elongating spermatids fail to mature further, whereas *Jam-C*$^{-/-}$ round spermatids lose cell polarity, and most of *Jam-C*$^{-/-}$ elongated spermatids are completely lost. RA175 and Jam-C seem to have similar but distinct functional roles during spermatid differentiation. Here we show that the cell polarity protein Par-3 with PDZ domains, a binding partner of Jams, is one of the associated proteins of the cytoplasmic region of RA175 in testis. Par-3 and Jam-C are partly co-localized with RA175 in the elongating and elongated spermatids; their distributions overlapped with that of RA175 on the tips of the dorsal region of the head of the elongating spermatid (steps 9 to 12) in the wild type. In the *Ra175*$^{-/-}$ elongating spermatid, Par-3 was absent, and Jam-C was absent or abnormally localized. The RA175 formed a ternary complex with Jam-C via interaction with Par-3. The lack of the ternary complex in the *Ra175*$^{-/-}$ elongating spermatid may cause the defect of the specialized adhesion structures, resulting in the oligo-astheno-teratozoospermia. *(Am J Pathol 2007, 171:1800–1810; DOI: 10.2353/ajpath.2007.070261)*

Epithelial cells have distinct apical and basolateral membrane domains separated by tight junctions (TJs). Junctional adhesion molecules (Jams), members of immunoglobulin superfamily with PDZ-binding domain, are localized at TJs and are involved in the establishment of epithelial cell polarity.[1–3] Jams associate with cell polarity protein Par-3 [partitioning defective-3, atypical PKC (aPKC) isotype-specific interacting protein (ASIP)][4–8] via its C-terminal PDZ-binding domain and recruit Par-3/Par-6/aPKC complex to nascent cell-cell contacts.[9–15]

In testis, two junctional complexes form near the base of Sertoli cells, Sertoli-Sertoli TJ and spermatid-Sertoli cell junction. The Sertoli-Sertoli TJ divides the microenvironment into the basal and adluminal compartment, whereas the spermatid-Sertoli cell junction retains the elongated spermatids in the invagination of Sertoli cells, which provides spermatogenic cells with essential signals and nutrients. Cell adhesion molecules such as Nectin-2 and Nectin-3, Jam-C, and RA175 (IGSF4A/RA175/TSLC1/SynCAM/SgIGSF/Necl2)[16–24] are members of the immunoglobulin superfamily with PDZ-binding domains, are involved in the spermatid-Sertoli cell junction, and are necessary for spermatid differentiation.[20,25–29]

Nectin-2 on the Sertoli cells heterophilically interacts with Nectin-3 on the elongated spermatid, and they are linked to the cytoskeletal structures and considered to be involved in the ectoplasmic specialization between sper-

Supported in part by the Ministry of Education, Science, and Sports (research grant 17-10 for nervous and mental disorders and grant-in-aid for scientific research on priority areas 18700333).

Accepted for publication August 16, 2007.

Supplemental material for this article can be found on *http://ajp.amjpathol.org*.

Address reprint requests to Momoi Takashi, National Institute of Neuroscience, NCNP, Oawahigashi-machi 4-1-1, Kodaira, Tokyo 187-8502, Japan. E-mail: momoi@ncnp.go.jp.

matids and Sertoli cells.[25,26] *Nectin-2*$^{-/-}$ male mice display a random disorganization of the spermatozoan head and midpiece attributable to overall disorganization of cytoskeletal structures, but they still possess motile spermatozoa,[25–27] whereas *Nectin-3*$^{-/-}$ mice show only defects of sperm morphogenesis.[28]

In contrast with Nectins, Jam-C or RA175 deficiency causes the loss of elongated spermatid. On the heads of elongated spermatids, Jam-C is confined to the junctional plaques specialized into adhesion structures that anchor spermatids to the Sertoli cell epithelium.[29] *Jam-C* deficiency (*Jam-C*$^{-/-}$) disrupts the cell polarity and acrosome structure of round spermatid and the localization of junctional plaques and induces almost complete loss of elongated spermatids.[29]

RA175 has a type II PDZ-binding domain (EYFI) at its C terminus,[16–24] which has calcium-independent, homophilic *trans*-cell adhesion activity, is expressed in the developing mouse nervous system and epithelia of various tissues, including testis.[16,19,20,23,24] We showed previously that *Ra175*-deficient (*Ra175*$^{-/-}$) male mice are infertile and show oligo-astheno-teratozoospermia; early elongating spermatids (steps 9 to 12) are impaired and fail to mature further.[20] RA175 is an essential molecule in forming and maintaining spermatid-Sertoli cell junction, which is necessary for the spermatid differentiation. In contrast with *Jam-C*$^{-/-}$ testis, the round spermatids (steps 1 to 8) are morphologically normal in the *Ra175*$^{-/-}$ testis. So RA175 and Jam-C seem to have similar but distinct functional roles during spermatid differentiation. However, little is known how RA175-mediated spermatid-Sertoli cell junction is formed.

To elucidate the role of the RA175 in the spermatid differentiation, we searched for proteins that associate with the cytoplasmic portion of RA175 by pull-down assay. Here we found that Par-3 is one of the associated molecules of cytoplasmic portion of RA175 and forms a ternary complex with Jam-C and RA175 and that *Ra175* deficiency alters distribution of Jam-C and Par-3 on the elongating spermatid, which causes oligo-astheno-teratozoospermia.

Materials and Methods

Plasmid Construct

cDNA fragments encoding RA175C (amino acids 402 to 456) and RA175ΔC (lacking C-terminus EYFI, amino acids 402 to 452) were amplified by polymerase chain reaction (PCR) using the following primers: forward primer for RA175C and RA175ΔC; 5′-GGATCCAGACATAAAGGTAC-3′, reverse primer for RA175C; 5′-GGATCCCTAGATGAAGTACTC-3′, reverse primer for RA175ΔC; 5′-GGATCCCTATTTCTTTTCTTCGGAGTTG-3′. PCR products were amplified by 1 cycle of 95°C for 2 minutes, 10 cycles of 95°C for 30 seconds and 62°C for 1 minute, and 1 cycle at 72°C for 7 minutes. PCR products were cloned into pGEM-T easy vector (Promega, Madison, WI) and then subcloned in-frame into *Bam*H1 site of the GST-tagged pEF-BOS[30] mammalian expression vector (pEB-GST). In addition, these cDNA fragments were subcloned into the *Bam*H1 site of pGEX-4T-3 vector (Pharmacia, Buckinghamshire, UK) and pMAL-c2X vector (New England Biolabs, Beverly, MA) for preparation of fusion protein with GST and maltose-binding proteins (MBPs), respectively.

cDNA of SRHis-rat Par-3 (SRHis-Par-3)[9] and GST-rat Par-3 PDZ fusion proteins [GST-Par-3-PDZ (1, 2, 3) (amino acids 237 to 708), GST-Par-3-PDZ (1, 2) (amino acids 237 to 589), GST-Par-3-PDZ (2, 3) (amino acids 402 to 708), and GST-Par-3-PDZ 2 (amino acids 402 to 589)][9] and pcDNA4-mouse Jam-C[31] were used for immunoprecipitation and pull-down experiments.

Preparation of Fusion Proteins

The purification of GST and MBP fusion proteins was performed as described in the manufacturers' manuals. GST-RA175C, GST-RA175ΔC, GST-Par-3 (1, 2, 3), GST-Par-3-PDZ (1, 2), GST-Par-3-PDZ (2, 3), and GST-Par-3 PDZ 2 fusion proteins were expressed in *Escherichia coli* BL21 (F^-, *omp* T, *hsd* S (r_B^-, m_B^-), *gal dcm*; Amersham Pharmacia Biotech, Buckinghamshire, UK). Expression of recombinant proteins was induced by 0.5 mmol/L isopropyl-D-thiogalactopyranoside for 2 hours. GST fusion proteins were isolated by glutathione Sepharose 4B beads affinity chromatography (GE Health Care Biosciences, Buckinghamshire, UK), and a part of the proteins was eluted with 50 mmol/L Tris-HCl (pH 8.0) containing 10 mmol/L glutathione. RA175C and MBP-RA175ΔC fusion proteins were expressed in *E. coli* TB1 (New England Biolabs). MBP fusion proteins were isolated by amylose resin affinity chromatography (New England Biolabs) and eluted with the buffer (20 mmol/L Tris-HCl, 200 mmol/L NaCl, 1 mmol/L ethylenediaminetetraacetic acid, 1 mmol/L azide, 1 mmol/L dithiothreitol) containing 10 mmol/L maltose. The GST fusion proteins and MBP fusion protein-bound beads were analyzed by sodium dodecyl sulfate-polyacrylamide gel electrophoresis and Coomassie brilliant blue staining and used for pull-down assay.

Pull-Down Assay

Pull-Down Assay Using Fusion Proteins

For direct binding assays, MBP-RA175C and -RA175ΔC fusion proteins (2 μg) were incubated with GST-Par-3 (2 μg)-conjugated glutathione Sepharose 4B beads in the buffer (20 mmol/L Tris-HCl, 150 mmol/L NaCl, 1% Triton X-100, 1 mmol/L ethylenediaminetetraacetic acid, 1 mmol/L dithiothreitol, the protease inhibitor cocktail, and 1 mmol/L phenylmethyl sulfonyl fluoride) for 12 hours at 4°C. After beads were washed five times with the same buffer, the bound proteins were released from beads by 50 mmol/L Tris-HCl (pH 8.0) containing 10 mmol/L glutathione and subjected to immunoblot analysis using rabbit anti-MBP (New England Biolabs) and monoclonal mouse anti-GST (Santa Cruz Biotechnology, Santa Cruz, CA).

Pull-Down Assay Using Peptide-Conjugated Sepharose Beads

Interaction between Par-3 and PDZ-binding motif of RA175C was examined by pull-down assay using peptide-conjugated beads. GST-Par-3-PDZ (1, 2, 3), GST-Par-3-PDZ (1, 2), GST-Par-3-PDZ (2, 3), and GST-Par-3-PDZ (2) were incubated with C-terminal peptide of RA175 (QNNSEEKKEYFI)-conjugated EAH Sepharose 4B beads (GE Health Care) in the 50 mmol/L Tris-HCl (pH7.5) containing 0.1% bovine serum albumin, 0.05 mol/L NaCl, 0.05% Triton X-100 for 6 hours at 4°C. After the beads were washed with the same buffer, the bound proteins were eluted by 0.1 mol/L glycine-HCl (pH 2.5) and subjected to the immunoblot analysis using monoclonal mouse anti-GST.

Pull-Down Assay for RA175C-Binding Proteins in Testis

Testes of 12-week-old wild-type male mice were lysed with lysis buffer (20 mmol/L Tris-HCl, pH 7.5, 150 mmol/L NaCl, 1% Triton X-100, 1 mmol/L ethylenediaminetetraacetic acid, 1 mmol/L dithiothreitol, the protease inhibitor cocktail, and 1 mmol/L phenylmethyl sulfonyl fluoride). The supernatant was incubated with GST-RA175C and/or GST-RA175ΔC (2 μg)-conjugated glutathione Sepharose 4B beads for 12 hours at 4°C. After beads were washed five times with the buffer, the bound proteins were released from beads by 50 mmol/L Tris-HCl (pH 8.0) containing 10 mmol/L glutathione and were subjected to immunoblot analysis using rabbit anti-RA175C,[18] and rabbit anti-Par-3,[9] rabbit anti-Jam-C,[32] and monoclonal mouse anti-GST, respectively. The amount of tubulin in the lysates was monitored by immunoblot analysis using monoclonal mouse anti-tubulin (Santa Cruz Biotechnology).

Transfection and Immunoprecipitation

Immunoprecipitation was performed as previously described.[18] COS cells were grown in α-minimum essential medium (Sigma, St. Louis, MO) with 10% fetal bovine serum, at 37°C in a humidified atmosphere of 5% CO_2. pEB-GST-RA175C (2 to 4 μg), pEB-GST-RA175ΔC (2 to 4 μg), SRHis-Par-3 (3 to 4 μg), pcDNA4-Jam-C (2 μg), and vacant vector (pcDNA4; Invitrogen, Carlsbad, CA) were co-transfected in COS cells by Lipofectamine 2000 (Promega) according to the manufacturer's specimen. COS cells were lysed with lysis buffer. Cell lysates were clarified by centrifugation at 15,000 rpm for 30 minutes. Par-3 and its associated proteins were immunoprecipitated by monoclonal mouse anti-Omni-probe (6His) (anti-His; Santa Cruz Biotechnology) or monoclonal mouse anti-GST. RA175, Par-3, and Jam-C in the immunoprecipitates were detected by immunoblot analysis using rabbit anti-RA175C, rabbit anti-Omni-probe (6His) (anti-His; Santa Cruz Biotechnology), and rabbit anti-Jam-C, respectively.

Immunoblot Analysis

Testes of 12-week-old *Ra175*$^{+/+}$ and *Ra175*$^{-/-}$ male mice were lysed with buffer (20 mmol/L Tris-HCl, 150 mmol/L NaCl, 0.1% Nonidet P-40, 1 mmol/L ethylenediaminetetraacetic acid, 10% glycerol, 5 mmol/L $MgCl_2$, 1 mmol/L phenylmethyl sulfonyl fluoride). After centrifugation at 15,000 rpm for 30 minutes, the cell extracts (50 μg of protein) were subjected to sodium dodecyl sulfate-polyacrylamide gel (7.5 to 12%) electrophoresis and immunoblot analysis using rabbit anti-RA175C, rabbit anti-Par-3, and rabbit anti-Jam-C, respectively.

Immunohistochemical Staining

Testes of 10- to 12-week-old *Ra175*$^{+/+}$ and *Ra175*$^{-/-}$ male mice were fixed in 2% paraformaldehyde in phosphate-buffered saline (PBS) at 4°C overnight and then soaked in 30% sucrose/PBS at 4°C overnight and embedded in Optimal Cutting Temperature (O.C.T.) compound (Sakura Finetec, Torrance, CA) and frozen. Frozen sections (10 μm thick) were cut on a cryostat and attached to MAS-coated slides (Matsunami Glass). Sections were immunostained with rabbit anti-Par-3, rabbit anti-Par-6B,[15] rabbit anti-Jam-C, goat anti-Jam-C (R&D Systems, Minneapolis, MN), rabbit anti-RA175C, chick anti-SynCAM, and monoclonal rat anti-Nectin-3 (MBL, Nagoya, Japan), rabbit anti-Tiam1, and anti-Cdc42, monoclonal mouse anti-Cdc42 (Santa Cruz Biotechnology), monoclonal mouse anti-PKCι (BD Bioscience, San Jose, CA) in PBS containing 0.1% skim milk and 0.1% Triton X-100 at 4°C for 2 days as described previously.[18] To confirm the specific immunoreactivity of anti-Par-3, the immunostaining was performed in the presence or absence of GST-Par-3 (amino acid 712 to 936) protein (10 μg/ml).[9] Alexa Fluor 488- and Alexa Fluor 568-conjugated secondary antibodies against mouse, rabbit, and rat IgG were purchased from Molecular Probes (Eugene, OR). Anti-Cy3-conjugated-chicken IgY was purchased from Chemicon, Temecula, CA. Acrosome structure was detected by fluorescein isothiocyanate (FITC)-conjugated peanut agglutinin (PNA) (J- Oilmills) staining in place of PAS staining. F-actin was detected by Alexa Fluor 488-phalloidin (Molecular Probes). Nuclei were detected by Hoechst 33342 at 37°C for 15 minutes. The reactivity was viewed using a confocal laser-scanning microscope (CSU-10, Yokogawa).

Conventional Reverse Transcriptase (RT)-PCR

Total RNA was prepared from testes of 12-week-old *Ra175*$^{+/+}$ and *Ra175*$^{-/-}$ male mice by RNeasy mini kit (Qiagen, Valencia, CA) according to the manufacturer's specifications. Complementary DNAs were synthesized from total RNA (1 μg) using reverse transcriptase (Invitrogen, Carlsbad, CA) as described previously.[33] cDNAs were subjected to conventional RT-PCR as described in the manual from Perkin-Elmer using the following primers: mouse Par-3 forward primer; 5′-CCCATGATGACGTGGGATTC-3′, and reverse primer; 5′-GAG AACCGGATCAACATCT-3′, mouse Jam-C forward primer; 5′-ACAGCTCG-

TACAC AATGAAC-3′, and reverse primer; 5′-TACTTGCATTCGCTTCCCAG-3′, mouse RA175 forward primer; 5′-CCACGTAACTTGATGATCGA-3′, and reverse primer; 5′-GATGAGCAAGCATAGCATGG-3′, and G3PDH

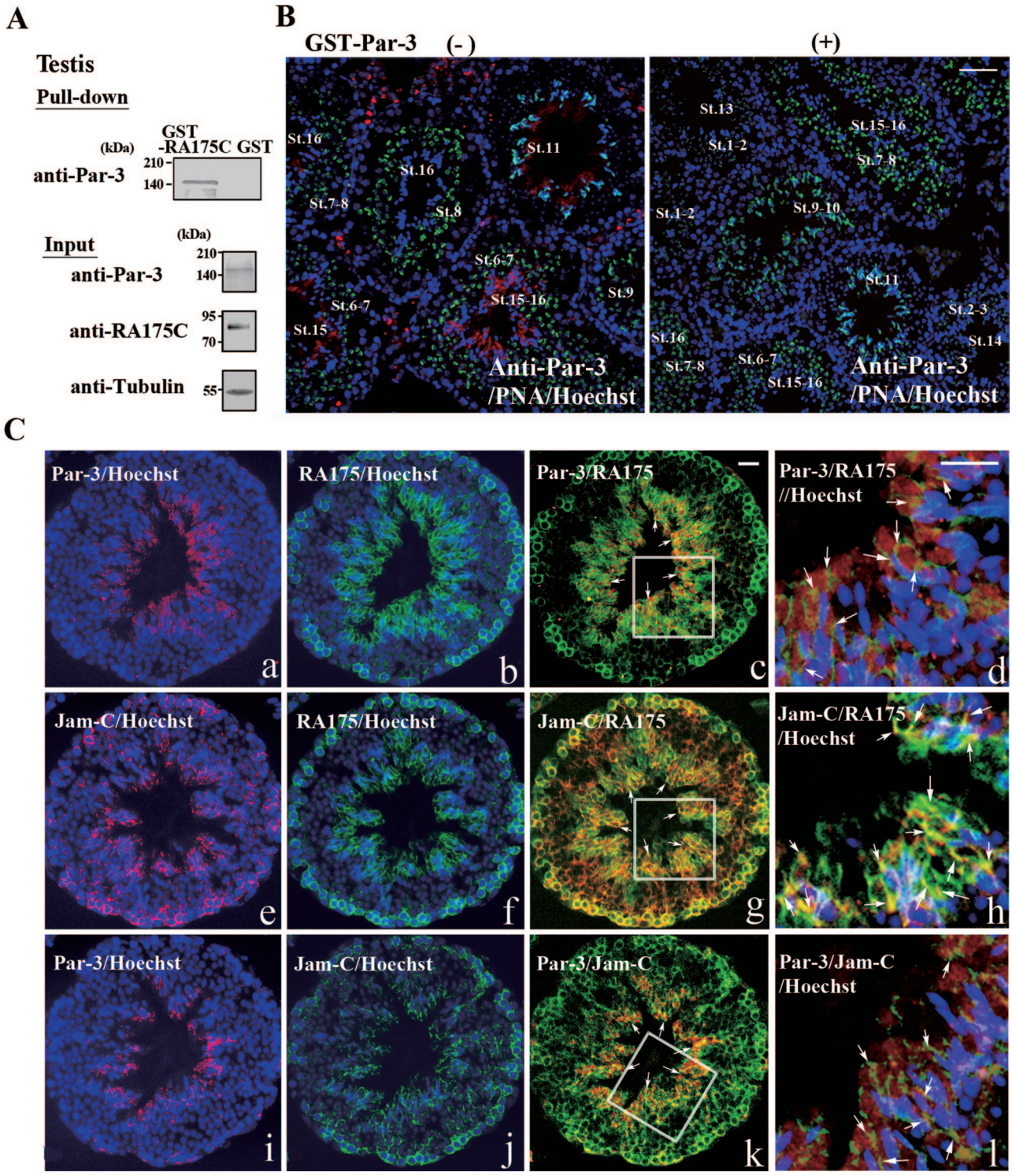

Figure 1. The distribution of Par-3 in mouse testis. **A:** Interaction between RA175 and Par-3 in mouse testis shown by pull-down assay. Par-3 (150 kDa) was detected in the testis proteins associated with RA175C by immunoblot using anti-Par-3. Input shows the amount of Par-3, Jam-C, and RA175 in the 1/10-fold volume of the cellular lysate, which was loaded for the pull-down experiment. **B:** Anti-Par-3 immunoreactivity in the testis. Anti-Par-3 immunoreactivity of mouse testes in the absence (**left**) and presence (**right**) of GST-Par-3 proteins. Red: anti-Par-3 immunoreactivity; green: PNA staining; blue: Hoechst. **C:** Co-localization of Par-3, Jam-C, and RA175 immunoreactivity in mouse testes at steps 11 to 12 (stage XI to XII). **a–d:** Par-3 and RA175 immunoreactivities. Red: rabbit anti-Par-3; green: chicken anti-SynCAM. **e–h:** Jam-C and RA175 immunoreactivities. Red: rabbit anti-Jam-C; green: chicken anti-SynCAM. **i–l:** Par-3 and Jam-C immunoreactivities. Red: rabbit anti-Par-3; green: goat anti-Jam-C; blue: Hoechst. **Arrows** indicate Par-3- and RA175-positive cells (**c**, **d**), Jam-C- and RA175-positive cells (**g**, **h**), and Par-3- and Jam-C-positive cells (**k**, **l**). **d**, **h**, and **l** are high magnifications of square regions in **c**, **g**, and **k**, respectively. Scale bars: 100 μm (**B**); 40 μm (**C**).

(Toyobo, Osaka, Japan). The PCR fragments were amplified as follows: 1 cycle at 95°C for 2 minutes, 30 cycles at 98°C for 20 seconds and 62°C for 1 minute, and 1 cycle at 72°C for 10 minutes. The RT-PCR products were electrophoresed on 2% NuSieve agarose gels (FM Bioproducts, Rockland, ME).

Real-Time PCR

Real-time PCR analysis was performed by Applied Biosystems 7500 fast real-time PCR system (Applied Biosystems, Foster City, CA) using the same primer for the conventional RT-PCR. The TaqMan probes for mouse Par-3 and Jam-C are as follows: carboxyfluorescein (FAM)-labeled mouse Par-3 probe; 5′-TGACTCAGCCGACTGCTCATTGAG-3′, and FAM-labeled mouse Jam-C probe; 5′-TATTACTGCGAAGCCCGGAACTC-3′. VIC-labeled mouse Gapd (VIC-labeled MGD probe, primer limited; Applied Biosystems) was used for endogenous control. The real-time PCR fragments were amplified as follows: 1 cycle at 95°C for 20 seconds, 60 cycles at 95°C for 3 seconds and 60°C for 30 seconds.

Results

We searched for proteins with PDZ domains that associate with the cytoplasmic portion of RA175 (RA175C), using a pull-down assay and immunoblot analysis. One of the molecules was Par-3 (150 kDa), a major isoform in testis,[9,34] which has three PDZ domains (Figure 1A). We compared the distribution of Par-3 in testis with the distribution of PNA staining, a marker for acrosome structure in the round and elongating spermatids.[29] Anti-Par-3 immunoreactivity was almost undetectable in spermatogonia, spermatocytes, and round spermatids but was detectable in elongating and elongated spermatids (steps 9 to 16) (Figure 1B, left), and this immunostaining in the elongating and elongated spermatids was completely blocked in the presence of exogenous Par-3 proteins (Figure 1B, right). RA175 was localized in spermatocytes and elongating (steps 9 to 12), and elongated spermatids (steps 13 to 16) in the testis.[20] RA175 co-localized with Jam-C in most of the elongating spermatids (Figure 1C, e–h), whereas Par-3 partly co-localized with RA175 and Jam-C in the elongating spermatids (Figure 1C, a–d and i–l). Their

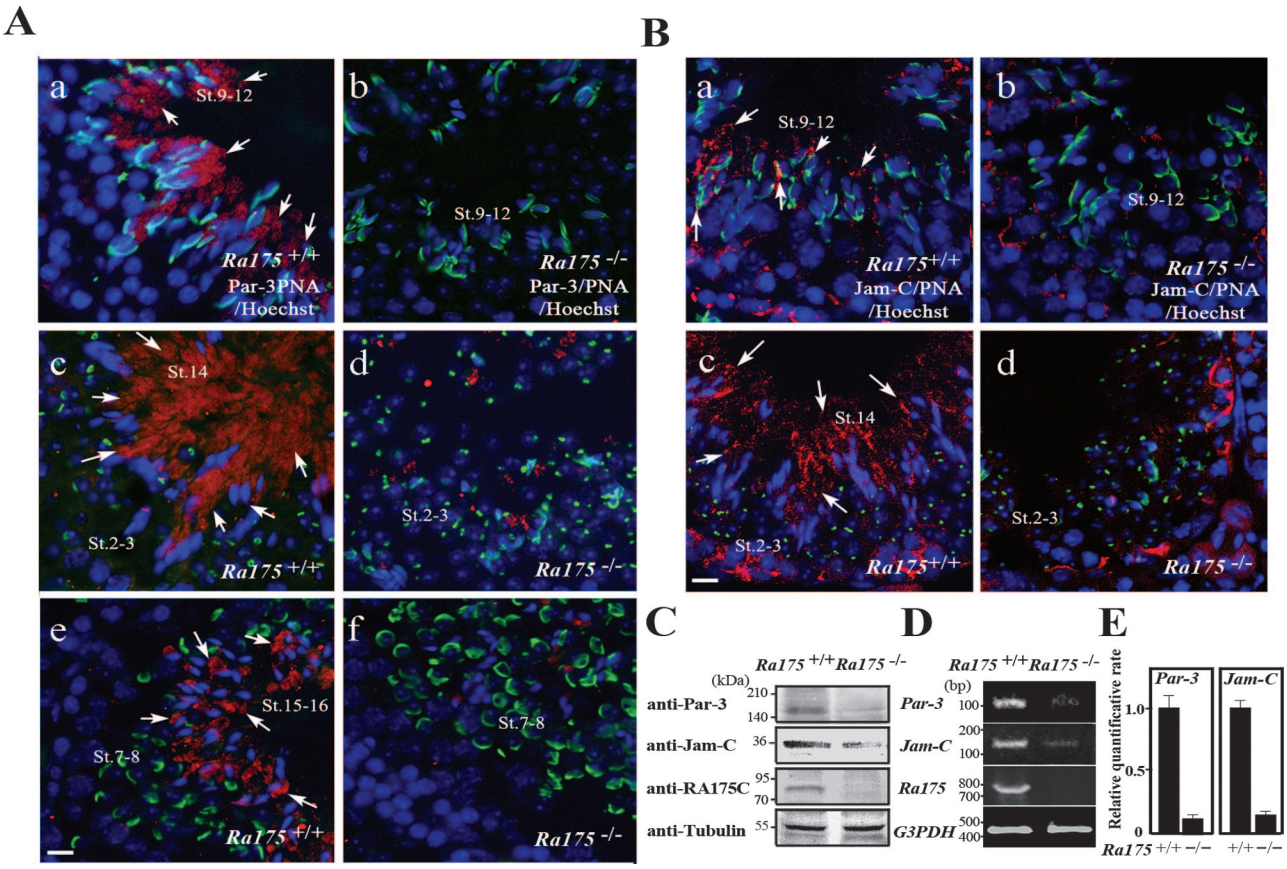

Figure 2. The expression of Par-3 and Jam-C and their distribution in *Ra175*$^{-/-}$ testis. **A:** Localization of Par-3 during the differentiation from round to elongated spermatids in *Ra175*$^{+/+}$ and *Ra175*$^{-/-}$ testes. **a**, **c**, **e:** *Ra175*$^{+/+}$; **b**, **d**, **f:** *Ra175*$^{-/-}$. Merged images of spermatids stained with anti-Par-3 (red), FITC-conjugated PNA staining (green), and Hoechst staining (blue). **a** and **b:** Steps 9 to 12 (stage IX to XII); **c:** steps 2 to 3, 14 (stage II/III); **d:** steps 2 to 3, 9 to 12 (stage IX to II/III); **e** and **f:** steps 7 to 8, 15 to 16 (stage VII). Most of Par-3 was lacked and only small amount of Par-3 was detected in the *Ra175*$^{-/-}$ testes. **B:** Localization of Jam-C on the elongating and elongated spermatid of in *Ra175*$^{+/+}$ and *Ra175*$^{-/-}$ testes. **a** and **b:** Steps 9 to 12 (stage IX to XII); **c:** Steps 2 to 3, 14 (stage II/III); **d:** steps 2 to 3, 9 to 12 (stage IX to II/III). **C:** Immunoblot analysis for Par-3 and Jam-C proteins in the extracts of *Ra175*$^{+/+}$ and *Ra175*$^{-/-}$ testis. **D:** Conventional RT-PCR analysis for Par-3 and Jam-C mRNA. **E:** Real-time PCR analysis for Par-3 and Jam-C mRNA. Columns indicate relative quantification rates. Error bars indicate SD. Scale bars = 20 μm.

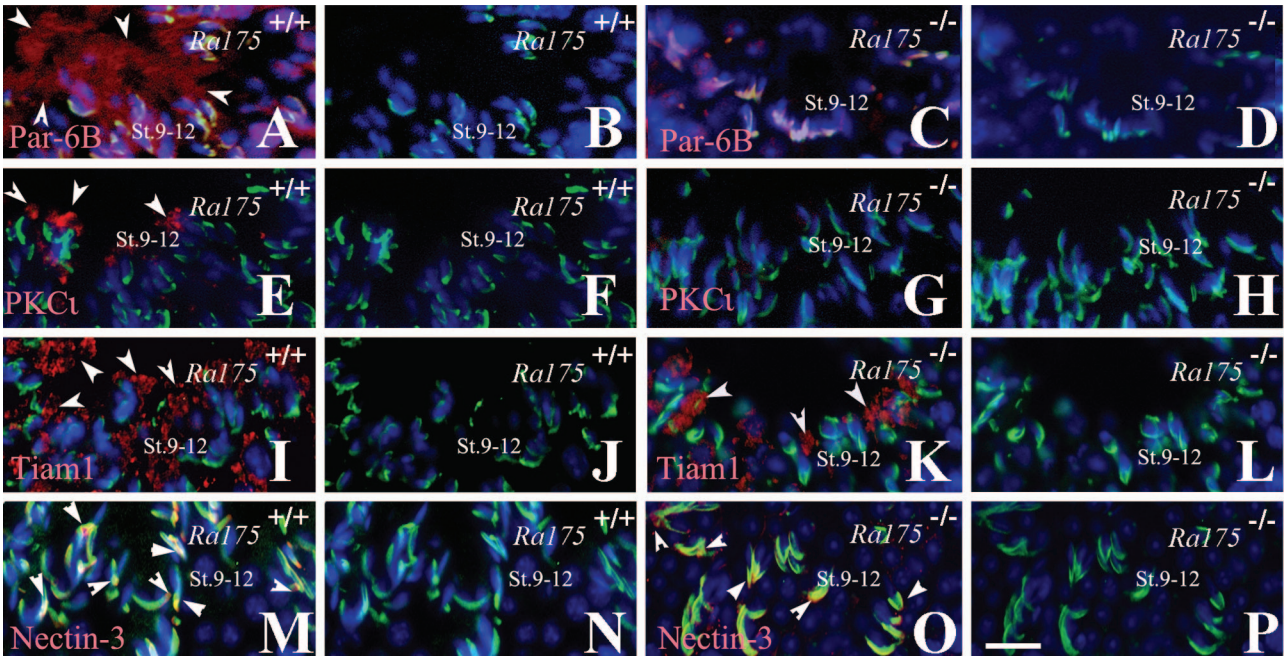

Figure 3. Localization of Par-6B, PKCι, Tiam1, and Nectin-3 in *Ra175*$^{+/+}$ and *Ra175*$^{-/-}$ testes. **A**, **B**, **E**, **F**, **I**, **J**, **M**, **N:** *Ra175*$^{+/+}$; **C**, **D**, **G**, **H**, **K**, **L**, **O**, **P:** *Ra175*$^{-/-}$. **A–D:** Par-6B; **E–H:** PKCι; **I–L:** Tiam1; **M–P:** Nectin-3. **A**, **C**, **E**, **G**, **I**, **K**, **M**, **O:** Merged images of spermatids stained with anti-Par-6B, -PKCι, -Tiam1, or -Nectin-3 (red), and FITC-conjugated PNA (green), and Hoechst staining (blue). **B**, **D**, **F**, **H**, **J**, **L**, **N**, **P:** Merged images stained with FITC-conjugated PNA (green), and Hoechst staining (blue). Stage IX to XII. **Arrowheads** indicate their positive immunoreactivities of elongating spermatids. Scale bar = 20 μm.

co-localization was also partly observed in the elongated spermatid (unpublished data). These results suggest that they function cooperatively during spermiogenesis.

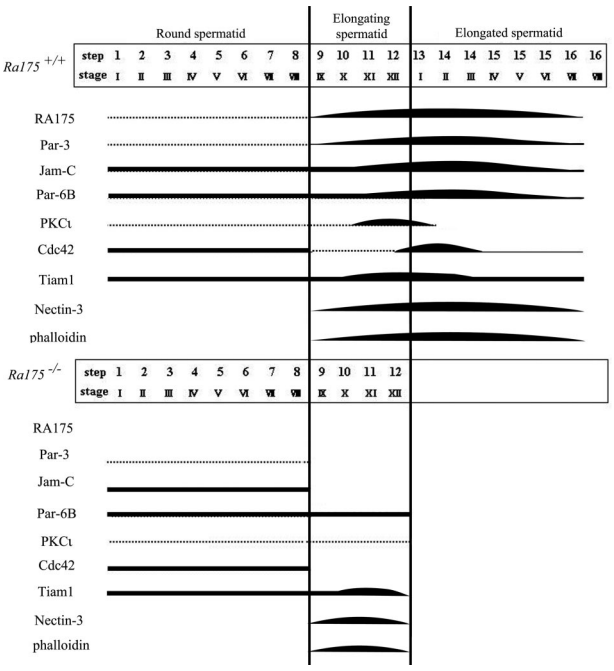

Figure 4. The distribution of Par-3, Jam-C, Par-6B, PKCι, Tiam1, and Nectin-3 in the germ cells in the testis were summarized. The expression of Par-3, Jam-C, Par-6B, PKCι, Tiam1, Cdc42, Nectin-3, and phalloidin reactivity were shown by bold bars. Par-3, Par-6B, PKCι were undetectable in the elongating spermatids (steps 9 to 12) in the *Ra175*$^{-/-}$ testis but only small number of their positive elongated spermatids appeared at step 13, probably because of the abnormal differentiation caused by *Ra175* deficiency. The fluorescence intensity was measured by the fluoromicroscopy imaging system AF6000 (Leica).

We examined the expression and distribution of Par-3 in the *Ra175*$^{+/+}$and *Ra175*$^{-/-}$ testis (Figure 2). Immunostaining showed the loss of the elongated spermatids (steps 13 to 16) expressing Par-3 in the *Ra175*$^{-/-}$ testis (Figure 2A). Par-3 was detected in the elongating spermatids (steps 9 to 12) (Figure 2Aa), abundant in the elongated spermatids (steps 13 to 15) (Figure 2Ac), and then decreased in the elongated spermatids (step 16) (Figure 2Ae) in the *Ra175*$^{+/+}$ testis. In contrast, Par-3 was rarely detected in the *Ra175*$^{-/-}$ testis because of the loss of the elongated spermatids (Figure 2A, b, d, and f) and was absent in the elongating spermatids impaired (steps 9 to 12) (Figure 2Ab);[20] most Par-3 was absent in the *Ra175*$^{-/-}$ testis except for the remaining small population (Figure 2Ad), probably the abnormally differentiated elongated spermatids before exfoliation or being phagocytosed.[20] Jam-C was almost lost from the elongating spermatids (steps 9 to 12; Figure 2B, a and b) and the elongated spermatids (step 14; Figure 2B, c and d) except for a few elongating spermatids but not from the spermatocytes of the *Ra175*$^{-/-}$ testis. Consistent with the immunostaining data, the amounts of Par-3 and Jam-C proteins and mRNAs were decreased in the *Ra175*$^{-/-}$ testis (Figure 2, C–E); Par-3 (150 kDa) prominently decreased in the *Ra175*$^{-/-}$ testis. Compared with the reduction of Par-3, that of Jam-C protein was not remarkable, probably attributable to the expression of Jam-C in the spermatocytes in the *Ra175*$^{-/-}$ testis. However, quantitative real-time PCR analysis showed ~90% reduction of Jam-C mRNA level as well as Par-3 mRNA level in the *Ra175*$^{-/-}$ testis.

Reduction of the Par-3 in the *Ra175*$^{-/-}$ testis seems not only attributable to the loss of elongated sperma-

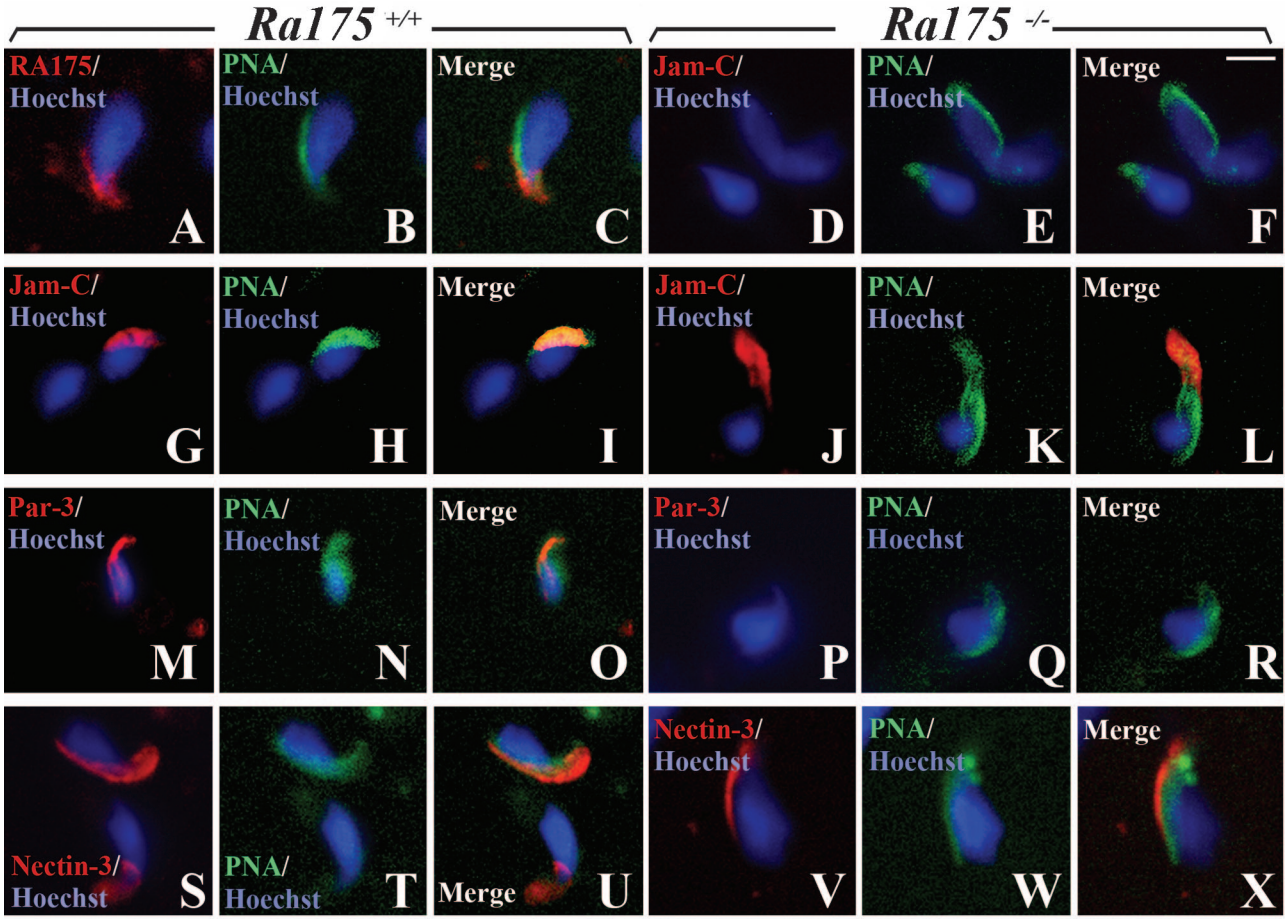

Figure 5. Co-localization of RA175, Par-3, Jam-C, and Nectin-3 in the elongating spermatids (step 9 to 12) of the *Ra175*$^{+/+}$ testis and loss of their co-localization in the *Ra175*$^{-/-}$ testis. **A–C**, **G–I**, **M–O**, **S–U:** *Ra175*$^{+/+}$; **D–F**, **J–L**, **P–R**, **V–X:** *Ra175*$^{-/-}$. **A–C:** Anti-RA175C; **D–F**, **G–I**, **J–L:** anti-Jam-C; **M–O**, **P–R:** anti-Par-3; and **S–X:** anti-Nectin-3. **A**, **D**, **G**, **J**, **M**, **P**, **S**, **V:** Images of spermatids stained with antibodies (red) and Hoechst staining (blue). **B**, **E**, **H**, **K**, **N**, **Q**, **T**, **W:** Images of spermatids stained with FITC-conjugated PNA (green), and Hoechst staining (blue). **C**, **F**, **I**, **L**, **O**, **R**, **U**, **X:** Merged images of spermatids stained with antibody (red), FITC-conjugated PNA (green), and Hoechst staining (blue). Jam-C and Par-3 immunoreactivities (**D** and **P**) were not detected in the dorsal region of the head of elongating spermatids except for some abnormal localization of Jam-C (**J**). Scale bar = 5 μm.

tids but also attributable to the impairment of the elongating spermatids. To make clear whether the absence of Par-3 on the elongating spermatids (steps 9 to 12) is closely associated with the impairment of the elongating spermatid, leading to the abnormal spermatid differentiation and resulting in the loss of the elongated spermatids, we examined the distributions of components of functional cell polarity complex Par-3 such as Par-6B, PKCι, in the *Ra175*$^{+/+}$ and *Ra175*$^{-/-}$ elongating spermatids (steps 9 to 12) (Figure 3, A–H). Par-6B and PKCι were present in the *Ra175*$^{+/+}$ elongating spermatids (steps 9 to 12) but most of them were absent in the *Ra175*$^{-/-}$ elongating spermatids (Figure 3, A–D and E–H). Tiam1, guanine nucleotide exchange factor for the Rho-like GTPase Rac, which is known to interact with Par-3/Par-6/aPKC complex via Par-6 and Par-3,[35] was detected in the *Ra175*$^{+/+}$ and *Ra175*$^{-/-}$ elongating spermatids (steps 9 to 12) (Figure 3, I–L). Nectin-3 was also present in the *Ra175*$^{+/+}$ and *Ra175*$^{-/-}$ elongating spermatids (Figure 3, M–P).

These results and the distribution of RA175, Nectin-3, and Jam-C in the *Ra175*$^{+/+}$ and *Ra175*$^{-/-}$ testis are summarized in Figure 4. In the *Ra175*$^{-/-}$ testis, the immunoreactivities of Jam-C, Par-6B, and PKCι as well as Par-3 were remarkably reduced. Thus, the absence of Par-3, Par-6B, and PKCι is closely associated with not only the loss of the *Ra175*$^{-/-}$ elongated spermatids (steps 13 to 16) but also the impairment of the *Ra175*$^{-/-}$ elongating spermatids (steps 9 to 12).

To understand the relationship between RA175, Jam-C, and Par-3 in the establishment of the adhesion structure on the elongating spermatids, we examined the distribution of RA175, Jam-C, and Par-3 on the head region of the PNA-positive elongating spermatids (steps 9 to 12) of *Ra175*$^{+/+}$ and *Ra175*$^{-/-}$ testis in more detail (Figure 5). RA175 was detected at the tips of the heads of *Ra175*$^{+/+}$ elongating spermatids (Figure 5, A–C). Jam-C staining overlapped with the PNA staining on the dorsal region of the heads of *Ra175*$^{+/+}$ elongating spermatids (Figure 5, G–I) as described previously,[29] whereas Jam-C was absent from the heads of most *Ra175*$^{-/-}$ elongating spermatids (Figure 5, D–F) or localized on the tips of the abnormally elongated heads of some of the *Ra175*$^{-/-}$ elongating spermatids (Figure 5, J–L). In contrast to Jam-C, Nectin-3 was detected in the dorsal region of the *Ra175*$^{+/+}$

Table 1. Expression of RA175, Par-3, Jam-C, and Nectin-3 in the Elongating Spermatids of the *Ra175*$^{+/+}$ Testis and the *Ra175*$^{-/-}$ Testis

Elongating spermatids (steps 9 to 12)		
Mouse genotype	*Ra175*$^{+/+}$	*Ra175*$^{-/-}$
RA175	+	−
Par-3	+	−
Jam-C	+	−/+ (abnormal shape)
Nectin-3	+	+

elongating spermatids (Figure 5, S–U) and similarly localized in the *Ra175*$^{-/-}$ elongating spermatids (Figure 5, V–X). Par-3 localized similarly to RA175 at the tips of the heads of *Ra175*$^{+/+}$elongating spermatids (Figure 5, M–O) but was not detected in the *Ra175*$^{-/-}$ elongating spermatids (Figure 5, P–R). Thus, unlike Nectin-3, Par-3 was absent and Jam-C was absent or abnormally localized on the *Ra175*$^{-/-}$ elongating spermatids impaired (Table 1).

We examined the region of RA175C that interacts with Par-3 by immunoprecipitation. RA175ΔC, RA175 lacking four C-terminal amino acids (EYFI), failed to interact with Par-3 (Figure 6A). These results suggest that interaction between RA175C and Par-3 is specifically mediated by the binding of the EYFI-PDZ domain. Furthermore, pull-down assay showed that MBP-RA175C directly bound with GST-Par-3 but MBP-RA175ΔC did not (Figure 6B), whereas RA175C-terminal peptide (12 amino acids) containing EYFI

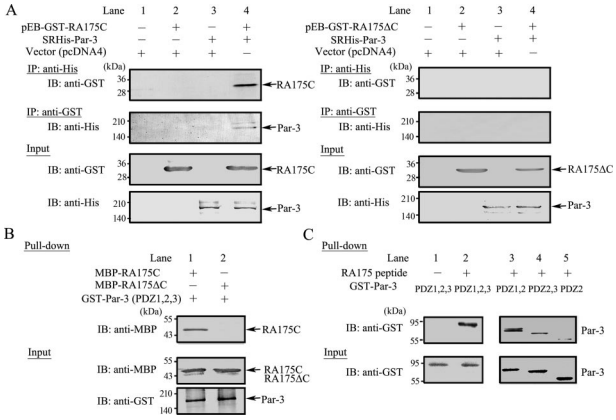

Figure 6. Involvement of PDZ-binding motif in the interaction between RA175C and Par-3. **A:** Immunoprecipitation analysis for interaction between RA175C or RA175ΔC lacking EYFI and Par-3. pEB-GST-RA175C (**left**) or pEB-GST-RA175ΔC (**right**) was co-transfected with or without SRHis-Par-3 in COS cells. The cell lysate was immunoprecipitated by anti-His or anti-GST. GST-RA175C or -RA175ΔC in the anti-His immunoprecipitates and His-Par-3 in the anti-GST immunoprecipitate were detected by immunoblot analysis using anti-GST and anti-His, respectively. A complex of RA175C and Par-3 was detected in the immunoprecipitate, but a complex of RA175ΔC and Par-3 was not. **B:** Pull-down assay for involvement of EYFI in the direct interaction between RA175C and Par-3. MBP-RA175C or MBP-RA175ΔC were incubated with GST-Par-3 (PDZ1, 2, 3)-conjugated Sepharose beads. The bound RA175 or RA175ΔC was examined by immunoblot analysis using anti-MBP. **C:** Pull-down assay using RA175C-terminal peptide. **Left:** Direct interaction between RA175C-terminal peptide and Par-3. GST-Par-3 (1, 2, 3) was incubated with Sepharose-beads (**lane 1**) and RA175C-terminal peptide-conjugated Sepharose beads (**lane 2**). **Right:** The domain of Par-3 interacting with RA175C-terminal peptide. The GST-PDZ (1, 2) (**lane 3**), -PDZ (2, 3) (**lane 4**), and -PDZ (2) (**lane 5**) were incubated with RA175C peptide-conjugated Sepharose beads. The bound Par-3 and its domains were detected by immunoblot analysis using anti-GST.

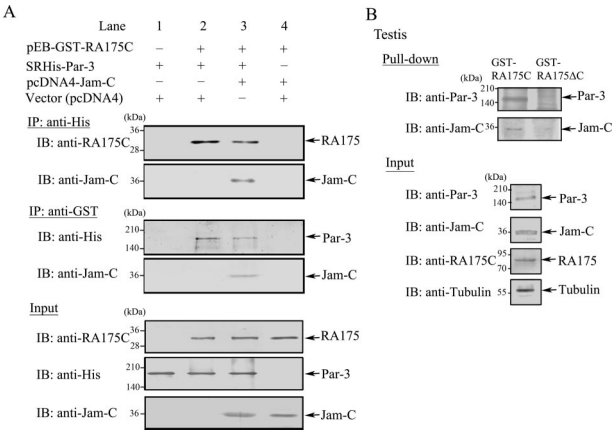

Figure 7. The ternary complex with RA175, Par-3, and Jam-C. **A:** Immunoprecipitation analysis for ternary complex. pEB-GST-RA175C and pcDNA4-Jam-C were co-transfected with or without SRHis-Par-3 into COS cells and the complex was immunoprecipitated by anti-His or anti-GST. RA175, Par-3, and Jam-C in the immunoprecipitate were detected by immunoblot analysis using anti-RA175C, anti-His, and anti-Jam-C, respectively. **B:** Pull-down assay for the ternary complex of RA175, Par-3, and Jam-C in mouse testis. The lysates of the mouse testis were incubated with GST-RA175- and GST-RA175ΔC-coupled Sepharose beads. The bound Par-3 and Jam-C were examined by immunoblot analysis using anti-Par-3 and anti-Jam-C, respectively.

directly bands with Par-3 (Figure 6C). RA175C-terminal peptide more preferentially interacted with PDZ(1, 2) than PDZ(2, 3) or PDZ(2). Thus, RA175 directly and specifically bound with Par-3 via EYFI-PDZ1 interaction.

To elucidate the relationship between RA175, Jam-C, and Par-3, we examined the interactions between RA175C, Jam-C, and Par-3 (Figure 7). RA175C interacted with Par-3. RA175C also interacted with Jam-C in the presence of Par-3 but not in the absence of Par-3 (Figure 7A). Thus, Par-3 interacted with both RA175 and Jam-C and formed a ternary complex with them (RA175/Par-3/Jam-C). Furthermore, both Jam-C and Par-3 were detected in the testis proteins associated with RA175C but not in those with RA175ΔC lacking EYFI (Figure 7B), suggesting that RA175 also formed a ternary complex of RA175/Par-3/Jam-C via EYFI in testis.

Discussion

The Distinct Roles of Cell Adhesion Molecules during Spermatid Differentiation

Homozygous null males of *Nectin-2* (*Nectin-2*$^{-/-}$), *Nectin-3* (*Nectin-3*$^{-/-}$), *Jam-C*$^{-/-}$, and *Ra175*$^{-/-}$ are infertile,[20,25,27–29] suggesting that cell adhesion molecules with PDZ-binding domains are involved in the spermatid-Sertoli cell junction and necessary for the spermatid differentiation. The sperm of these model mice are malformed and are morphologically similar to abnormal sperm seen in some cases of human male infertility, suggesting that they are useful for analyzing the molecular bases of these human conditions.

In the *Ra175*$^{-/-}$ testis, the elongating spermatids (steps 9 to 12) are impaired and fail to mature further and show oligo-astheno-teratozoospermia.[20] Nectin-3 and phalloidin-positive F-actin normally localized on the *Ra175*$^{-/-}$

elongating spermatids (steps 9 to 12) (Figure 3 and see Supplementary Figure 1, see *http://ajp.amjpathol.org*), suggesting that RA175 and Nectins are independently involved in the establishment of the spermatid-Sertoli cell junction. Thus, unlike *Nectin-2*$^{-/-}$ and/or *Nectin-3*$^{-/-}$ testis, disorganization of cytoskeletal structure is not a cause of the impairment of the elongating spermatids in the *Ra175*$^{-/-}$ testis.

In contrast to *Nectin-2*$^{-/-}$, *Nectin-3*$^{-/-}$, and *Ra175*$^{-/-}$ male mice, *Jam-C*$^{-/-}$ male mice have an almost complete loss of elongated spermatids as a result of a defect in the polarization of adhesion junctions on the round and elongating spermatids.[29] In the *Ra175*$^{-/-}$ elongating spermatids (steps 9 to 12), Jam-C distribution was absent or abnormal (Figures 2 and 5). Thus, these cell adhesion molecules have similar but distinct functional roles during spermatid differentiation. RA175 and Jam-C seem to be functionally associated in the establishment of the adhesion structures on the elongating spermatids.

Decrease of Par-3, a Binding Partner of Jam-C, in the Ra175$^{-/-}$ *Testis*

In addition to Jam-C, Par-3 was also decreased in the *Ra175*$^{-/-}$ testis, probably attributable to the loss of the elongated spermatids (steps 13 to 16) expressing Par-3 and Jam-C in the *Ra175*$^{-/-}$ testis (Figures 1 and 2). However, Par-3 and its functional Par-3/Par-6B/aPKCι complex as well as Jam-C were absent in the *Ra175*$^{-/-}$ elongating spermatids (steps 9 to 12) (Figures 3 and 5 and Table 1), suggesting the possibility that *Ra175* deficiency specifically induces the loss of Jam-C/Par-3 complex on the elongating spermatids (steps 9 to 12), resulting in the abnormal spermatid differentiation and loss of the elongated spermatids (steps 13 to 16).

There are two possible explanations for the absence of Par-3 immunoreactivity on the elongating spermatids (steps 9 to 12) of the *Ra175*$^{-/-}$ testis (Figure 5, Table 1). One is that *Ra175* deficiency decreases the expression of Par-3 and Jam-C in the elongating spermatids. However, Jam-C persists in the spermatocytes in the *Ra175*$^{-/-}$ testis (Figure 2B), suggesting that this possibility is less likely. The other possible explanation is that *Ra175* deficiency alters the localization of Par-3 in the elongating spermatids. In the developing epithelial tissues, Par-3 shows strong immunoreactivity on the TJ but not in the cytoplasm. Par-3 or Par-3/Par-6B/aPKCι complex that is not associated with RA175 in the elongating spermatids (steps 9 to 12) of the *Ra175*$^{-/-}$ testis may be labile and sensitive to degradation or may have a conformation not detected by the immunostaining.

RA175/Par-3/Jam-C Ternary Complex on the Head of Elongating Spermatids

Jam-C associated with RA175C in the presence of Par-3 (Figure 7), suggesting that they form ternary complex of RA175/Par-3/Jam-C. Par-3 has three PDZ domains, and RA175 and Jam-C may have the ternary complex via binding with different PDZ binding domains of Par-3.[4–8] However, RA175 as well as Jam-C preferentially bound with PDZ1 of Par-3[4] (Figure 6C) and Par-3 forms oligomer by self-association,[36] suggesting that they form ternary complex via competitive binding of RA175 and Jam-C to multiple PDZ1s of the self-associate oligomeric Par-3.

Jam-C is confined to the junctional plaques on the heads of round and elongating spermatids.[29] The absence of Par-3 and the altered localization or lack of Jam-C on the head of the *Ra175*$^{-/-}$ elongating sperma-

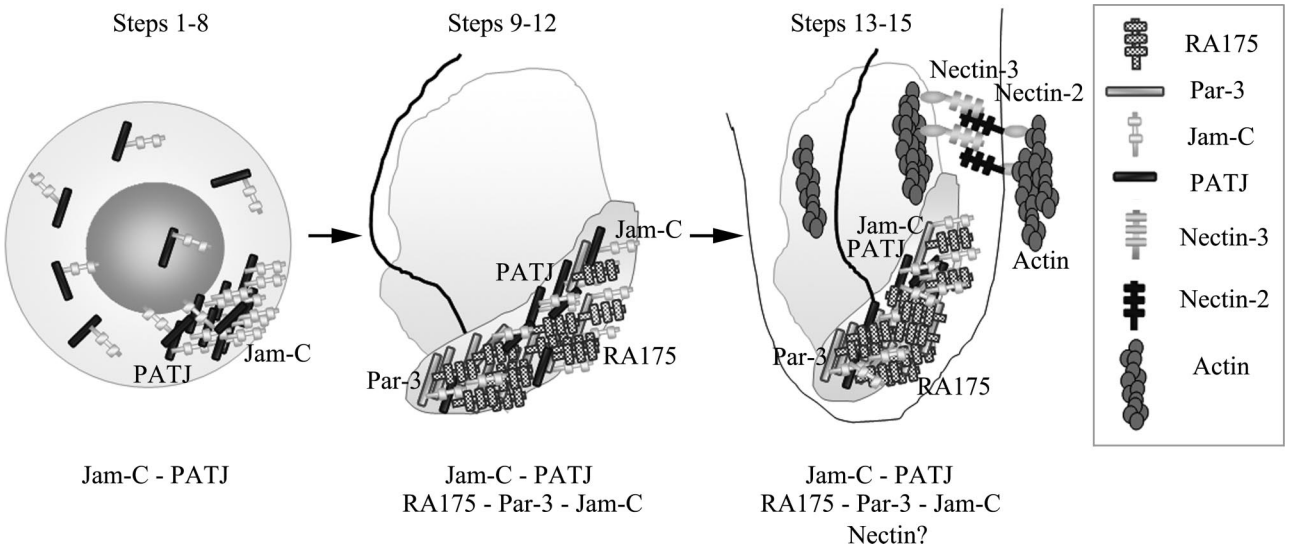

Figure 8. The interaction between RA175, Jam-C, and Par-3 and scheme of a ternary complex on the elongating spermatids. Ternary complex of RA175, Jam-C, and Par-3 on the elongating spermatids (steps 9 to 12). In the *Ra175*$^{-/-}$ testis, Par-3 and Jam-C localization is not polarized on the elongating spermatids and differentiation into elongated spermatids is defective (steps 13 to 15), as shown in *Jam-C*$^{-/-}$ testes.[29] PDZ-binding domain at Cterminus of RA175 plays a role in the recruitment of Par-3 to the Jam-C localized on the surface membrane of the head region of the elongating spermatids. The functional cooperation of Jam-C, RA175, and Par-3 on the spermatid head may be necessary for the further maturation of the elongating spermatids.

tids (Figure 5) suggests that RA175 also affects the interaction between Jam-C and Par-3 on the head of the elongating spermatids. RA175 appears to be involved in the recruitment of Par-3 to Jam-C on the head of the elongating spermatids to form a ternary complex of RA175/Par-3/Jam-C (Figure 8). The *Ra175*$^{-/-}$ elongating spermatids may fail to recruit Par-3/Par-6B/PKCι complex to the anterior part of the head, resulting in the abnormal adhesion structures and cell junctions on the elongating spermatids, subsequently abnormal differentiation and loss of the elongated spermatids.

The Molecular Mechanism of the Adhesion Structure on the Elongating Spermatid

The localization of RA175, Par-3, Par-6B, PKCι, and Jam-C on the head of the elongating spermatids suggests that RA175 can play a role in the recruitment of the Par-3/Par-6B/PKCι complex to the specialized adhesion structures on the elongating spermatids (steps 9 to 12) via the RA175/Par-3/Jam-C complex (Figure 8). We detected very weak immunoreactivity of Par-3 in the round spermatids (Figure 1). This discrepancy between our data and the data of Gliki and colleagues[29] on the distribution of Par-3 in the round spermatids may be attributable to the different quality of antibodies used. However, it is possible that a tiny amount of the ternary complex of RA175/Par-3/Jam-C may also be present in the round spermatids and may participate in the cell polarity of round spermatids although this complex mainly functions in the elongating spermatids.

Jam-C binds to the PDZ domain of PATJ (PALS1-associated TJ protein), a multi-PDZ domain protein,[29] which plays a central role in the recruitment of the Crb3 (Crumb-3)/PALS1 (protein associated with Lin seven 1)/PATJ to the adhesion structures,[37–39] and Jam-C colocalizes with PATJ on the round spermatids.[29] Crb3/PALS1/PATJ and Par-3/Par-6/aPKC complexes may cooperate to form the spermatid-Sertoli cell junction on the round and or elongating spermatids via association with Jam-C (Figure 8). This may be one of the reasons why the elongating spermatids are impaired in the *Ra175*$^{-/-}$ as well as the *Jam-C*$^{-/-}$ testis or why loss of Jam-C in the *Ra175*$^{-/-}$ and *Jam-C*$^{-/-}$ testis may cause the impairment in elongating spermatids.

We conclude that RA175 is essential in forming and maintaining elongated spermatid-Sertoli cell junction, through its participation in a functional complex with Jam-C and Par-3 that polarizes the cell junction on the elongating spermatids.

Acknowledgments

We thank Dr. Shigeki Yuasa, Dr. Kiyotaka Toshimori, and Dr. Atsushi Suzuki for valuable scientific discussion; and Dr. Masato Mori for real-time PCR analysis.

References

1. Aurrand-Lions M, Duncan L, Ballestrem C, Imhof BA: JAM-2, a novel immunoglobulin superfamily molecule, expressed by endothelial and lymphatic cells. J Biol Chem 2001, 276:2733–2741
2. Bazzoni G: The JAM family of junctional adhesion molecules. Curr Opin Cell Biol 2003, 15:525–530
3. Martìn-Padura I, Lostaglio S, Schneemann M, Williams L, Romano M, Fruscella P, Panzeri C, Stoppacciaro A, Ruco L, Villa A, Simmons D, Dejana E: Junctional adhesion molecule, a novel member of the immunoglobulin superfamily that distributes at intercellular junctions and modulates monocyte transmigration. J Cell Biol 1998, 142:117–127
4. Ebnet K, Suzuki A, Horikoshi Y, Hirose T, Meyer zu Brickwedde MK, Ohno S, Vestweber D: The cell polarity protein ASIP/Par-3 directly associates with junctional adhesion molecule (JAM). EMBO J 2001, 20:3738–3748
5. Ebnet K, Aurrand-Lions M, Kuhn A, Kiefer F, Butz S, Zander K, Meyer zu Brickwedde MK, Suzuki A, Imhof BA, Vestweber D: The junctional adhesion molecule (JAM) family members JAM-2 and JAM-3 associate with the cell polarity protein Par-3: a possible role for JAMs in endothelial cell polarity. J Cell Sci 2003, 116:3879–3891
6. Ebnet K, Suzuki A, Ohno S, Vestweber D: Junctional adhesion molecules (JAMs): more molecules with dual functions? J Cell Sci 2004, 117:19–29
7. Itoh M, Sasaki H, Furuse M, Ozaki H, Kita T, Tsukita S: Junctional adhesion molecule (JAM) binds to Par-3: a possible mechanism for the recruitment of Par-3 to tight junctions. J Cell Biol 2001, 154:491–497
8. Schneeberger EE, Lynch RD: The tight junction: a multifunctional complex. Am J Physiol 2004, 286:C1213–C1228
9. Izumi Y, Hirose T, Tamai Y, Hirai S, Nagashima Y, Fujimoto T, Tabuse Y, Kemphues KJ, Ohno S: An atypical PKC directly associates and colocalizes at the epithelial tight junction with ASIP, a mammalian homologue of Caenorhabditis elegans polarity protein Par-3. J Cell Biol 1998, 143:95–106
10. Joberty G, Petersen C, Gao L, Macara IG: The cell-polarity protein Par6 links Par3 and atypical protein kinase C to Cdc42. Nat Cell Biol 2000, 2:531–539
11. Lin D, Edwards AS, Fawcett JP, Mbamalu G, Scott JD, Pawson T: A mammalian Par-3-Par-6 complex implicated in Cdc42/Rac1 and aPKC signalling and cell polarity. Nat Cell Biol 2000, 2:540–547
12. Nishimura T, Yamaguchi T, Kato K, Yoshizawa M, Nabeshima Y, Ohno S, Hoshino M, Kaibuchi K: PAR-6-PAR-3 mediates Cdc42-induced Rac activation through the Rac GEFs STEF/Tiam1. Nat Cell Biol 2005, 7:270–277
13. Ohno S: Intercellular junctions and cellular polarity: the Par-aPKC complex, a conserved core cassette playing fundamental roles in cell polarity. Curr Opin Cell Biol 2001, 13:641–648
14. Suzuki A, Ohno S: The Par-aPKC system: lessons in polarity. J Cell Sci 2006, 119:979–987
15. Yamanaka T, Horikoshi Y, Suzuki A, Sugiyama Y, Kitamura K, Maniwa R, Nagai Y, Yamashita A, Hirose T, Ishikawa H, Ohno S: Par-6 regulates aPKC activity in a novel way and mediates cell-cell contact-induced formation of the epithelial junctional complex. Genes Cells 2001, 6:721–731
16. Biederer T, Sara Y, Mozhayeva M, Atasoy D, Liu X, Kavalali ET, Sudhof TC: SynCAM, a synaptic adhesion molecule that drives synapse assembly. Science 2002, 297:1525–1531
17. Fujita E, Soyama A, Urase K, Mukasa T, Momoi T: RA175, which is expressed during the neuronal differentiation of P19 EC cells, temporally expressed during neurogenesis of mouse embryos. Neurosci Res 1998, 22:283
18. Fujita E, Soyama A, Momoi T: RA175, which is the mouse ortholog of TSLC1, a tumor suppressor gene in human lung cancer, is a cell adhesion molecule. Exp Cell Res 2003, 287:57–66
19. Fujita E, Urase K, Soyama A, Kouroku Y, Momoi T: Distribution of RA175/TSLC1/SynCAM, a member of the immunoglobulin superfamily, in the developing nervous system. Brain Res Dev Brain Res 2005, 154:199–209
20. Fujita E, Kouroku Y, Ozeki S, Tanabe Y, Toyama Y, Maekawa M, Kojima N, Senoo H, Toshimori K, Momoi T: Oligo-astheno-teratozoospermia in mice lacking RA175/TSLC1/SynCAM/IGSF4A, a cell ad-

hesion molecule in the immunoglobulin superfamily. Mol Cell Biol 2006, 26:718–726
21. Kuramochi M, Fukuhara H, Nobukuni T, Kanbe T, Maruyama T, Ghosh HP, Pletcher M, Isomura M, Onizuka M, Kitamura T, Sekiya T, Reeves RH, Murakami Y: TSLC1 is a tumor-suppressor gene in human non-small-cell lung cancer. Nat Genet 2001, 27:427–430
22. Shingai T, Ikeda W, Kakunaga S, Morimoto K, Takekuni K, Itoh S, Satoh K, Takeuchi M, Imai T, Monden M, Takai Y: Implications of nectin-like molecule-2/IGSF4/RA175/SgIGSF/TSLC1/SynCAM1 in cell-cell adhesion and transmembrane protein localization in epithelial cells. J Biol Chem 2003, 278:35421–35427
23. Urase K, Soyama A, Fujita E, Momoi T: Expression of RA175 mRNA, a new member of the immunoglobulin superfamily, in developing mouse brain. Neuroreport 2001, 12:3217–3721
24. Wakayama T, Koami H, Ariga H, Kobayashi D, Sai Y, Tsuji A, Yamamoto M, Iseki S: Expression and functional characterization of the adhesion molecule spermatogenic immunoglobulin superfamily in the mouse testis. Biol Reprod 2003, 68:1755–1763
25. Mueller S, Rosenquist TA, Takai Y, Bronson RA, Wimmer E: Loss of nectin-2 at Sertoli-spermatid junctions leads to male infertility and correlates with severe spermatozoan head and midpiece malformation, impaired binding to the zona pellucida, and oocyte penetration. Biol Reprod 2003, 69:1330–1340
26. Ozaki-Kuroda K, Nakanishi H, Ohta H, Tanaka H, Kurihara H, Mueller S, Irie K, Ikeda W, Sakai T, Wimmer E, Nishimune Y, Takai Y: Nectin couples cell-cell adhesion and the actin scaffold at heterotypic testicular junctions. Curr Biol 2002, 12:1145–1150
27. Bouchard MJ, Dong Y, McDermott BM Jr, Lam DH, Brown KR, Shelanski M, Bellve AR, Racaniello VR: Defects in nuclear and cytoskeletal morphology and mitochondrial localization in spermatozoa of mice lacking nectin-2, a component of cell-cell adherens junctions. Mol Cell Biol 2000, 20:2865–2873
28. Inagaki M, Irie K, Ishizaki H, Tanaka-Okamoto M, Miyoshi J, Takai Y: Role of cell adhesion molecule nectin-3 in spermatid development. Genes Cells 2006, 11:1125–1132
29. Gliki G, Ebnet K, Aurrand-Lions M, Imhof BA, Adams RH: Spermatid differentiation requires the assembly of a cell polarity complex downstream of junctional adhesion molecule-C. Nature 2004, 431:320–324
30. Mizushima S, Nagata S: pEF-BOS, a powerful mammalian expression vector. Nucleic Acids Res 1990, 18:5322
31. Aurrand-Lions M, Lamagna C, Dangerfield JP, Wang S, Herrera P, Nourshargh S, Imhof BA: Junctional adhesion molecule-C regulates the early influx of leukocytes into tissues during inflammation. J Immunol 2005, 174:6406–6415
32. Lamagna C, Hodivala-Dilke KM, Imhof BA, Aurrand-Lions M: Antibody against junctional adhesion molecule-C inhibits angiogenesis and tumor growth. Cancer Res 2005, 65:5703–5710
33. Fujita E, Kouroku Y, Urase K, Tsukahara T, Momoi MY, Kumagai H, Takemura T, Kuroki T, Momoi T: Involvement of Sonic hedgehog in the cell growth of LK-2 cells, human lung squamous carcinoma cells. Biochem Biophys Res Commun 1997, 238:658–664
34. Gao L, Macara IG, Joberty G: Multiple splice variants of Par3 and of a novel related gene, Par3L, produce proteins with different binding properties. Gene 2002, 294:99–107
35. Chen X, Macara IG: Par-3 controls tight junction assembly through the Rac exchange factor Tiam1. Nat Cell Biol 2005, 7:262–269
36. Mizuno K, Suzuki A, Hirose T, Kitamura K, Kutsuzawa K, Futaki M, Amano Y, Ohno S: Self-association of Par-3-mediated by the conserved N-terminal domain contributes to the development of epithelial tight junctions. J Biol Chem 2003, 278:31240–31250
37. Hurd TW, Gao L, Roh MH, Macara IG, Margolis B: Direct interaction of two polarity complexes implicated in epithelial tight junction assembly. Nat Cell Biol 2003, 5:137–142
38. Roh MH, Margolis B: Composition and function of PDZ protein complexes during cell polarization. Am J Physiol 2003, 285:R377–R387
39. Macara IG: Parsing the polarity code. Nat Rev Mol Cell Biol 2004, 5:220–231